

---

Faculty of Mathematical Sciences

University of Twente

University for Technical and Social Sciences

---

---

P.O. Box 217  
7500 AE Enschede

The Netherlands

Phone: +31-53-4893400

Fax: +31-53-4893114

Email: [memo@math.utwente.nl](mailto:memo@math.utwente.nl)

---

MEMORANDUM No. 1497

Singularities at rims in three-dimensional fluid flow

C.H. DRIESEN AND J.G.M. KUERTEN<sup>1</sup>

SEPTEMBER 1999

ISSN 0169-2690

---

<sup>1</sup>Faculty of Mechanical Engineering, Eindhoven University of Technology, P.O. Box 513, 5600 MB Eindhoven

# SINGULARITIES AT RIMS IN THREE-DIMENSIONAL FLUID FLOW

C.H. DRIESEN<sup>†</sup> AND J.G.M. KUERTEN<sup>‡</sup>

*Twente Institute of Mechanics, J.M. Burgers Centre*

*<sup>†</sup>Faculty of Mathematical Sciences*

*University of Twente, P.O. Box 217*

*7500 AE Enschede, The Netherlands*

*email: c.h.driesen@math.utwente.nl*

*<sup>‡</sup>Faculty of Mechanical Engineering*

*Eindhoven University of Technology, P.O. Box 513*

*5600 MB Eindhoven, The Netherlands*

*Keywords.* Stokes flow, Asymptotic approximations, Local singularities

*AMS.Class.* 32S05, 41A60, 76D07.

ABSTRACT. Asymptotic solutions are presented for Stokes flow near circular rims in three dimensional geometries. Using nonstandard toroidal coordinates, asymptotic analytical expressions are derived for different corner angles. In comparison to the two-dimensional case, an extra critical corner angle value is derived, below which the swirling behavior of a particle is absent. Illustrations of the motion of a particle near a rim in a three-dimensional fluid flow are given for different corner angles.

## 1. INTRODUCTION

In many practical applications of fluid flow geometries with sharp edges occur. Examples are flow near a cavity or around a protuberance mounted on a surface. Numerical simulations of these flows can suffer from inaccuracies caused by the singular behavior of the shear-stress components near the sharp edges. Knowledge of the singular behavior can be incorporated in the numerical method and thus increase the accuracy.

In two-dimensional flow problems geometries may contain sharp corners, as for example the corners of a cavity. Near these special geometric points the solutions of the viscous flow equations behave in a special way. Dependent on the shape the vorticity and the shear-stress components can become singular or an infinite number of vortices of decreasing strength can appear. For several relevant cases this behavior can be computed analytically by calculating the dominant contribution to the solution of the flow equations in a small neighborhood of the special point. This has been studied extensively in literature [9, 11, 12]. Moffatt also showed that, for viscous fluid flow problems, near sharp corners and rims the inertial terms are always negligible, thus resulting in the Stokes equations.

For Stokes flow near a separation point analytical solutions for problems in two and three dimensions are given in [10]. For three-dimensional geometries, analytical solutions for axisymmetric flow near a rim are known [2, 4]. For axisymmetric geometries analytical solutions are presented by Davis [3] and Hasimoto [7]. In their papers analytical formulations are given for flow over a circular hole in an infinitely thin plane wall. The analytical results of Davis are confirmed by the numerical computations of Pozrikidis [13, 14], who computed shear-stress components in the neighborhood of a circular rim with a boundary-integral method.

In this paper we derive analytical formulations for the solutions of the fluid flow equations in the neighborhood of a circular rim. A circular rim can be for example the rim of a cavity or an orifice in a plane wall, a plane wall with a hemisphere attached to it, or the rim of a circular disk. Since the calculated solutions are strongly related to the two-dimensional results, we first recall the two-dimensional case in the next section. In section 3 the three-dimensional geometry is studied.

## 2. SINGULARITY IN TWO DIMENSIONS

For the two-dimensional problem, a solution procedure is described as introduced by Lugt [9] and Moffatt [11]. This procedure starts with the biharmonic equation for the stream function and uses separation of variables in polar coordinates, which leads to an eigenvalue problem for the azimuthal coordinate. The boundary conditions on the edge determine the eigenvalues and subsequently the solutions for the radial coordinate. In this section we will summarize these results since they are employed in the three-dimensional calculations.

The Stokes equations and boundary conditions can be reformulated as

$$\nabla^4 \Psi = 0, \tag{2.1}$$

and

$$\Psi = \frac{\partial \Psi}{\partial \theta} = 0 \quad \text{if } \theta = \pm \gamma, \tag{2.2}$$

where  $\Psi$  denotes the stream function and polar coordinates are defined as shown in Fig. 1, where  $r$  is the distance to the corner,  $\theta$  is the angle from the point to the bisection, and  $2\gamma$  is the total angle of the corner. Starting from the assumption that  $\Psi(r, \theta) = R(r)\Theta(\theta)$  it is found that

$R(r) = r^{\lambda+1}$  and  $\Theta(\theta)$  satisfies the equation

$$\Theta'''' + 2(\lambda^2 + 1)\Theta'' + (\lambda^2 - 1)^2\Theta = 0, \quad (2.3)$$

where a prime denotes the derivative with respect to  $\theta$ . Together with the boundary conditions  $\Theta(\pm\gamma) = \Theta'(\pm\gamma) = 0$  this forms an eigenvalue problem. The separation variable,  $\lambda$ , which may be complex is called the eigenvalue. If only the differential equation for  $\Theta$  is considered, the following solutions are found [9, 11]:

$$\Theta = A \cos(\lambda + 1)\theta + B \sin(\lambda + 1)\theta + C \cos(\lambda - 1)\theta + D \sin(\lambda - 1)\theta, \text{ if } \lambda \neq 1, \quad (2.4)$$

and

$$\Theta = A \cos 2\theta + B \sin 2\theta + C\theta + D, \text{ if } \lambda = 1. \quad (2.5)$$

Solutions with  $\Re(\lambda) < 0$  are physically irrelevant since the velocity should remain finite for  $r \rightarrow 0$ . The vorticity near a sharp corner is singular for values of  $\lambda$  with  $\Re(\lambda) < 1$ . An example is shown in Fig. 2 where the solution has been computed with a method of series expansions [6]. We will denote these values as the singular values. To obtain equations for the eigenvalues  $\lambda$ , (2.4) is divided into so-called symmetric solutions with  $A$  and  $C$  equal to zero, and skew-symmetric solutions with  $B$  and  $D$  equal to zero [9]. For several angles  $2\gamma$  the smallest skew-symmetric eigenvalues  $\lambda_a$  and the smallest symmetric eigenvalues  $\lambda_s$  are given in Table 1.

For corner angles  $2\gamma \leq \pi$  no singular solutions can be found. There is one singular solution for corner angles  $\pi < 2\gamma \leq 1.4303\pi$  and there are two singular solutions for angles  $1.4303\pi < 2\gamma \leq 2\pi$ . For a corner angle  $2\gamma = 2\pi$ , which corresponds to an infinitely thin plate, there is one double singular solution. In [11] it is shown that for values  $2\gamma < 2\gamma_e$  with  $\gamma_e \approx 0.81287\pi$  all

$2\gamma$	$\lambda_a$	$\lambda_s$
$\pi/6$	$8.06297+i4.20287$	$14.33030+i5.19641$
$2\pi/6$	$4.05933+i1.95205$	$7.18196+i2.45567$
$3\pi/6$	$2.73959+i1.11902$	$4.80825+i1.46393$
$4\pi/6$	$2.09414+i0.60459$	$3.36307+i0.88123$
$5\pi/6$	$1.53386$	$2.93672+i0.36375$
$7\pi/6$	$0.75197$	$1.48581$
$8\pi/6$	$0.61573$	$1.14891$
$1.4303\pi$	$0.56829$	$1.00000$
$9\pi/6$	$0.54448$	$0.90853$
$10\pi/6$	$0.51222$	$0.73090$
$11\pi/6$	$0.50145$	$0.59819$
$2\pi$	$0.50000$	$0.50000$

TABLE 1. First two values of  $\lambda$  for a number of angles.

eigenvalues are complex. In order to find the real form of these solutions, we write the complex eigenvalue  $\lambda$  as

$$\lambda = \kappa_1 + i\kappa_2. \quad (2.6)$$

The  $r$ -dependent part of the solution can then be written as:

$$r^{\lambda+1} = r^{\kappa_1+1} [\cos(\kappa_2 \ln r) + i \sin(\kappa_2 \ln r)] \quad (2.7)$$

For  $r \rightarrow 0$  the terms  $\cos(\kappa_2 \ln r)$  and  $\sin(\kappa_2 \ln r)$  oscillate between -1 and +1 with ever increasing frequency. Hence, an infinite sequence of eddies will appear between the corner edges. An extended description of properties of these eddies can be found in [11]. In the next section we will see that in the three-dimensional situation, eddy structures will not appear if the angle becomes smaller than a certain value.

In boundary-element computations [1, 5, 8] the singular solutions can be employed in the integral equations.

### 3. SINGULARITY IN THREE DIMENSIONS

In general, in three dimensions the stream function does not exist, but the Stokes equations are equivalent to a fourth order differential equation for a vector function. Proceeding in a similar way as in two dimensions, we will derive solutions for the Stokes equations in the region close to the circular rim. This solution is valid if the distance to the rim is small compared to the radius of the circle. We will show that, in contrast to the two-dimensional case, eddy structures do not appear for small angles. As an example of a relevant geometry we can think of the circular rim of a cavity in a flat plate.

Since  $\nabla \cdot u = 0$  a solution vector function  $Y$  can be defined by

$$u = \nabla \times Y. \quad (3.8)$$

With this definition, the solutions will automatically satisfy the continuity equation. Taking the curl of the Stokes equations and substituting (3.8) results in

$$\nabla^{(4)} \times Y = 0, \quad (3.9)$$

where  $\nabla^{(4)}$  means that the curl is taken four times. We introduce special toroidal coordinates  $r, \theta$  and  $\varphi$  by

$$\begin{aligned} x &= r \sin \theta & 0 \leq r < a \\ y &= (a + r \cos \theta) \cos \varphi & \text{with } -\pi \leq \theta < \pi \\ z &= (a + r \cos \theta) \sin \varphi & 0 \leq \varphi < 2\pi \end{aligned} \quad (3.10)$$

where  $a$  is the radius of the circle. A sketch of the coordinate system is given by Fig. 3. Note that (3.10) does not define a global coordinate transformation but can only be used in a neighborhood of the rim. The boundary conditions are

$$u_r, u_\theta, u_\varphi = 0 \quad \text{at} \quad \theta = \pm\gamma, \quad (3.11)$$

where  $\gamma$  can be defined as in the two-dimensional case, and the  $u_r, u_\theta$  and  $u_\varphi$  are the components of  $u$  in the directions of the unit vectors. In a similar way as in electrodynamics, we can add a vector of the form  $Z = \nabla H$  to  $Y$  without affecting the velocity components  $u_r, u_\theta$  and  $u_\varphi$  given by (3.8). Without loss of generality we can choose  $H$  in such a way that the first element of  $Y$  becomes zero. Finding solutions for  $Y$  can thus be restricted to the second and third component. In a similar way as in the two-dimensional problem, we assume that the solution



vector  $Y$  consists of combinations of separate functions from the different variables

$$Y = \begin{bmatrix} 0 \\ r^{\lambda_2+1}\Theta_2(\theta)S_2(\varphi) \\ r^{\lambda_3+1}\Theta_3(\theta)S_3(\varphi) \end{bmatrix}. \quad (3.12)$$

We use the axisymmetry of the geometry to define two sets of solutions. One set of solutions with  $S_2(\varphi) = \sin(k\varphi)$  and  $S_3(\varphi) = \cos(k\varphi)$ , and the other set with  $S_2(\varphi) = \cos(k\varphi)$  and  $S_3(\varphi) = \sin(k\varphi)$ ,  $k = 0, 1, 2, \dots$ . The solution method is described for the first set of solutions. The procedure for the second set is very similar. In this section we will not compute analytical solutions of the problem, but restrict ourselves to asymptotic solutions which are valid for  $r \rightarrow 0$ . This means that we consider  $r/a$  as a small parameter and retain only the leading order terms in the computations. From (3.12) and (3.8) expressions for the velocity components for small  $r$  can be derived

$$\begin{bmatrix} u_r \\ u_\theta \\ u_\varphi \end{bmatrix} = \begin{bmatrix} (-\frac{k}{a}r^{\lambda_2+1}\Theta_2 + r^{\lambda_3}\Theta_3') \cos k\varphi \\ -(\lambda_3 + 1)r^{\lambda_3}\Theta_3 \cos k\varphi \\ (\lambda_2 + 2)r^{\lambda_2}\Theta_2 \sin k\varphi \end{bmatrix}. \quad (3.13)$$

Equations for the unknown functions  $\Theta_2(\theta)$  and  $\Theta_3(\theta)$  can be obtained from the  $r$ ,  $\theta$  and  $\varphi$  component of (3.9) by substitution of (3.12). We are searching for solutions close to the singular rim. Therefore, only the parts with the lowest order of  $r$  are important. If (3.12) is substituted and we distinguish the lowest orders of  $r$  for  $\lambda_2$  and  $\lambda_3$  from the higher order terms the equations can be written as:

$$\begin{aligned} r^{\lambda_2+1}[\lambda_2 + 2][\Theta_2'' + \lambda_2^2\Theta_2'] + O(r^{\lambda_2+2}) \\ - \frac{k}{a}r^{\lambda_3+2}[\lambda_3 - 1][\Theta_3'' + (\lambda_3 + 1)^2\Theta_3] + O(r^{\lambda_3+3}) = 0, \end{aligned} \quad (3.14)$$

for the  $r$ -component,

$$r^{\lambda_2+1}[\lambda_2 - 2][\lambda_2 + 2][\Theta_2'' + \lambda_2^2 \Theta_2] + O(r^{\lambda_2+2}) \\ + \frac{k}{a} r^{\lambda_3+2} [\Theta_3''' + (\lambda_3 + 1)^2 \Theta_3'] + O(r^{\lambda_3+3}) = 0, \quad (3.15)$$

for the  $\theta$ -part of the Stokes equations and

$$\frac{k}{a} r^{\lambda_2+2} [\Theta_2''' + \lambda_2^2 \Theta_2'] + O(r^{\lambda_2+3}) \\ - r^{\lambda_3+1} [\Theta_3''' + 2(\lambda_3^2 + 1)\Theta_3'' + (\lambda_3^2 - 1)^2 \Theta_3] + O(r^{\lambda_3+2}) = 0 \quad (3.16)$$

for the  $\varphi$ -component. The leading order solutions of these equations depend on the relation between  $\lambda_2$  and  $\lambda_3$ . For example in (3.14) both terms are only of the same order of magnitude if  $\Re(\lambda_2) = \Re(\lambda_3) + 1$ . If  $\Re(\lambda_2) < \Re(\lambda_3) + 1$  the first term is dominant and the resulting lowest order equation reads

$$\Theta_2''' + \lambda_2^2 \Theta_2' = 0. \quad (3.17)$$

If  $\Re(\lambda_2) > \Re(\lambda_3) + 1$  the second term dominates and we get

$$\Theta_3'' + (\lambda_3 + 1)^2 \Theta_3 = 0 \quad (3.18)$$

as leading order equation. Considering all three equations (3.14)-(3.16) we see that five different regions can be distinguished:

1.  $\Re(\lambda_3) < \Re(\lambda_2) - 1$
2.  $\Re(\lambda_3) = \Re(\lambda_2) - 1$
3.  $\Re(\lambda_2) - 1 < \Re(\lambda_3) < \Re(\lambda_2) + 1$
4.  $\Re(\lambda_3) = \Re(\lambda_2) + 1$
5.  $\Re(\lambda_3) > \Re(\lambda_2) + 1$

In the next subsections we will subsequently search for solutions in all these 5 cases.

**3.1. The case  $\Re(\lambda_3) < \Re(\lambda_2) - 1$ .** When only the lowest order quantities are taken into account, (3.14) results in (3.18), (3.15) results in the derivative of (3.18) and (3.16) results in (2.3) for  $\Theta_3(\theta)$ . The boundary conditions, which can be derived from (3.13) and (3.11), are

$$\Theta_3(\pm\gamma) = \Theta_3'(\pm\gamma) = 0. \quad (3.19)$$

It is easy to see that no solution can be found which satisfies the boundary conditions.

**3.2. The case  $\Re(\lambda_3) = \Re(\lambda_2) - 1$ .** A solution can only be found if  $\Im(\lambda_3) = \Im(\lambda_2)$ . Hence, we will look for solutions with  $\lambda_3 = \lambda_2 - 1$ . When only the lowest order quantities are taken into account, Eq. (3.14) results in

$$[\lambda_3 + 3][\Theta_2''' + (\lambda_3 + 1)^2\Theta_2'] - \frac{k}{a}[\lambda_3 - 1][\Theta_3'' + (\lambda_3 + 1)^2\Theta_3] = 0. \quad (3.20)$$

The  $\theta$ -component of the Stokes equations yields

$$[\lambda_3 - 1][\lambda_3 + 3][\Theta_2'' + (\lambda_3 + 1)^2\Theta_2] + \frac{k}{a}[\Theta_3''' + (\lambda_3 + 1)^2\Theta_3'] = 0, \quad (3.21)$$

and Eq. (3.16) gives

$$\Theta_3'''' + 2(\lambda_3^2 + 1)\Theta_3'' + (\lambda_3^2 - 1)^2\Theta_3 = 0. \quad (3.22)$$

This is Eq. (2.3) again, and we can conclude that the solution for  $\Theta_3$  is given by

$$\Theta_3 = A \cos(\lambda_3 + 1)\theta + B \sin(\lambda_3 + 1)\theta + C \cos(\lambda_3 - 1)\theta + D \sin(\lambda_3 - 1)\theta, \quad (3.23)$$

where  $A, B, C$  and  $D$  can be determined from the boundary conditions for  $u_r$  and  $u_\theta$  which are

$$\Theta_3(\pm\gamma) = \Theta_3'(\pm\gamma) = 0. \quad (3.24)$$

We can distinguish again between symmetric and skew-symmetric solutions, and find the same eigenfunctions for the different angles  $2\gamma$ . The only difference in the solution between two and three dimensions is that  $u_r$  and  $u_\theta$  are multiplied by a function of  $\varphi$ . Solution (3.23) can be substituted in (3.21) which results in

$$[\lambda_3 + 3][\Theta_2'' + (\lambda_3 + 1)^2 \Theta_2] + \frac{k}{a} 4\lambda_3 [-C \sin(\lambda_3 - 1)\theta + D \cos(\lambda_3 - 1)\theta] = 0. \quad (3.25)$$

It can be verified that substitution of (3.23) in (3.20) gives the derivative of (3.25) with respect to  $\theta$ . The solution of (3.25) is

$$\Theta_2 = E \cos(\lambda_3 + 1)\theta + F \sin(\lambda_3 + 1)\theta + \frac{k}{a(\lambda_3 + 3)} [C \sin(\lambda_3 - 1)\theta - D \cos(\lambda_3 - 1)\theta], \quad (3.26)$$

where  $C$  and  $D$  are the same constants as in (3.23) and  $E$  and  $F$  are arbitrary constants. With (3.13) an expression for  $u_\varphi$  can be obtained. After substitution of the boundary conditions for  $u_\varphi$ ,

$$\Theta_2(\pm\gamma) = 0, \quad (3.27)$$

the expression becomes

$$u_\varphi = \frac{k}{a} r^{\lambda_3+1} \left[ D \frac{\cos(\lambda_3 - 1)\gamma}{\cos(\lambda_3 + 1)\gamma} \cos(\lambda_3 + 1)\theta - D \cos(\lambda_3 - 1)\theta + C \sin(\lambda_3 - 1)\theta - C \frac{\sin(\lambda_3 - 1)\gamma}{\sin(\lambda_3 + 1)\gamma} \sin(\lambda_3 + 1)\theta \right] \sin k\varphi. \quad (3.28)$$

The values of  $\lambda_3$  are already determined by the boundary conditions for  $u_r$  and  $u_\theta$ . Eq. (3.28) is formulated in such a way that the boundary conditions for  $u_\varphi$  are automatically satisfied for every arbitrary angle. We can conclude that for every corner angle  $2\gamma$ , eigenvalues  $\lambda_3 = \lambda_2 - 1$  can be found. This does not imply that this is the lowest order solution for the velocity components

near a rim, because there might be other solutions with  $\Re(\lambda_3) > \Re(\lambda_2) - 1$ . We will discuss these solutions in the next subsections.

**3.3. The case  $\Re(\lambda_2) - 1 < \Re(\lambda_3) < \Re(\lambda_2) + 1$ .** If higher order terms are neglected in (3.14) to (3.16) then equation (3.15) results in:

$$\Theta_2'' + \lambda_2^2 \Theta_2 = 0, \quad (3.29)$$

and (3.14) results in the derivative of (3.29). The  $\varphi$ -component gives (3.22) again. The boundary conditions are given by (3.24) and (3.27). Eq. (3.29) gives for  $\Theta_2(\theta)$ :

$$\Theta_2(\theta) = A \cos \lambda_2 \theta + B \sin \lambda_2 \theta, \quad (3.30)$$

with  $A$  and  $B$  unknown coefficients. The possible values of  $\lambda_2$  can be obtained from the boundary conditions. For the symmetric solutions the function  $\Theta_2(\theta)$  can be written as

$$\Theta_2(\theta) = A \cos \lambda_2 \theta, \quad \lambda_2 = \frac{l\pi}{2\gamma}, \quad l = 1, 3, 5, \dots \quad (3.31)$$

The skew-symmetric solutions are defined by

$$\Theta_2(\theta) = B \sin \lambda_2 \theta, \quad \lambda_2 = \frac{l\pi}{\gamma}, \quad l = 1, 2, 3, \dots \quad (3.32)$$

We can conclude that only the symmetric solution can become singular for angles  $2\gamma > \pi$ . For  $\Theta_3(\theta)$  the solution is given by (3.23) again, with coefficients which are independent of  $\Theta_2(\theta)$ . In the prescribed interval for  $\lambda_2$  and  $\lambda_3$  the general solution of the velocity components is given by

$$\begin{bmatrix} u_r \\ u_\theta \\ u_\varphi \end{bmatrix} = \begin{bmatrix} r^{\lambda_3} \Theta_3'(\theta) \cos k\varphi \\ -(\lambda_3 + 1) r^{\lambda_3} \Theta_3(\theta) \cos k\varphi \\ r^{\lambda_2} \Theta_2(\theta) \sin k\varphi \end{bmatrix}. \quad (3.33)$$

The part of the solution for  $u_r$  from  $\Theta_2$  as it was presented in (3.13) is not included here, because we only retain the leading order terms in the expansion of the solution.

As an example that there exist angles for which  $Re(\lambda_2) - 1 < Re(\lambda_3) < Re(\lambda_2) + 1$  indeed, we can look at an angle  $2\gamma = 3\pi/2$ . Such an angle is present at the rim of a cylindrical cavity. For this angle, the smallest eigenvalue  $\lambda_3$  is equal to  $\lambda_3 \approx 0.54448$  while the smallest eigenvalue of  $\lambda_2$  is equal to  $2/3$ , which is in agreement with the prescribed interval.

**3.4. The case  $\Re(\lambda_3) = \Re(\lambda_2) + 1$ .** It can be shown that the solution presented in the previous subsection is also valid if  $\Re(\lambda_3) = \Re(\lambda_2) + 1$ . However, the values of  $\lambda_2$  and  $\lambda_3$  depend in different ways on the boundary conditions. This implies that there are only a limited amount of corner angles where this equality holds. The smallest eigenvalues  $\lambda$  are the so-called skewsymmetric values that can be computed from [9]

$$\sin(2\gamma\lambda) = -\lambda \sin(2\gamma). \quad (3.34)$$

To compute the angles where  $\Re(\lambda_3) = \Re(\lambda_2) + 1$  we substitute

$$\lambda_3 = \lambda_2 + 1 + iy = \frac{\pi}{2\gamma} + 1 + iy \quad (3.35)$$

in Eq. (3.34), where  $y$  is the imaginary part of  $\lambda_3$ . From the real and imaginary part the following equations for  $2\gamma$  and  $y$  can be derived

$$\sinh(2\gamma y) = y \tan(2\gamma), \quad (3.36)$$

and

$$2\gamma \cosh(2\gamma y) \sin(2\gamma) = (\pi + 2\gamma) \sin(2\gamma). \quad (3.37)$$

It is easy to see that  $2\gamma = \pi$  and  $2\gamma = 2\pi$  in combination with  $y = 0$  are solutions of (3.36) and (3.37). However, if we look for example for the resulting eigenvalue  $\lambda_3$  belonging to a corner angle  $2\gamma = 2\pi$ , we find that  $\lambda_3 = \frac{3}{2}$ . For such a corner angle, a smaller eigenvalue  $\lambda_3 = \frac{1}{2}$  exists. We want to find corner angles  $2\gamma$  where the resulting eigenvalue  $\lambda_3$  is the smallest possible eigenvalue. From (3.36) and (3.37) an expression for  $y$  can be obtained

$$y = \pm \frac{\sqrt{\left(\frac{\pi}{2\gamma} + 1\right)^2 - 1}}{\tan 2\gamma}, \quad 2\gamma \neq \pi, 2\pi \quad (3.38)$$

and after substitution of (3.38) in (3.36) the equation for  $2\gamma$  yields

$$\sinh \frac{2\gamma \sqrt{\left(\frac{\pi}{2\gamma} + 1\right)^2 - 1}}{\tan 2\gamma} = \sqrt{\left(\frac{\pi}{2\gamma} + 1\right)^2 - 1}. \quad (3.39)$$

We can conclude from (3.38) and (3.39) that, for every complex eigenvalue  $\lambda_3$ , the complex conjugate is an eigenvalue too. Eq. (3.39) has two solutions,  $2\gamma \approx 0.35481\pi$  and  $2\gamma \approx 1.44315\pi$ . However, the second solution does not result in the smallest possible eigenvalue  $\lambda_3$  for that corner angle. Therefore, the only solution of our interest is given by  $2\gamma_c \approx 0.35481\pi$ . The corresponding eigenvalue is equal to  $\lambda_3 \approx 3.81840 \pm i1.80804$ . We can conclude that for angles with  $2\gamma_c \leq 2\gamma \leq 2\pi$  the solution of the form (3.33) is the lowest order solution. For angles  $0 < 2\gamma < \gamma_c$  another solution can be found, which is shown in the next subsection.

**3.5. The case  $\Re(\lambda_2) + 1 < \Re(\lambda_3)$ .** In this subsection, we derive solutions for the velocities  $u_r$ ,  $u_\theta$  and  $u_\varphi$  in the prescribed region for  $\lambda_2$  and  $\lambda_3$ . In the previous subsection we found that this region corresponds with the angle interval  $0 < 2\gamma < 2\gamma_c$ . If higher order terms are neglected in (3.14) to (3.16) then equation (3.15) results in (3.29) again. Equations (3.14) and (3.16) result in the derivative of (3.29). The boundary conditions are

$$\Theta_2(\pm\gamma) = 0. \quad (3.40)$$

The general solution for the velocity components can be derived by (3.13) and is given by

$$\begin{bmatrix} u_r \\ u_\theta \\ u_\varphi \end{bmatrix} = A \begin{bmatrix} \frac{k}{a} r^{\lambda_2+1} \Theta_2(\theta) \cos k\varphi \\ 0 \\ -(\lambda_2 + 2) r^{\lambda_2} \Theta_2(\theta) \sin k\varphi \end{bmatrix}, \quad (3.41)$$

with  $\Theta_2(\theta)$  as defined in (3.30). As an example that there are angles for which  $Re(\lambda_2) + 1 < Re(\lambda_3)$  indeed, we consider an angle  $2\gamma = \pi/6$ . We can think of a sphere recessed in a plane, where  $2\gamma$  is the angle made by the surface of the sphere where it meets the plane. The smallest eigenvalue of  $\lambda_3$  of the solution  $\Theta_3(\theta)$  from the previous subsection is equal to  $\lambda_3 = 8.06297 + i4.20287$ , while the smallest eigenvalue from  $\Theta_2(\theta)$  for this angle, which comes from the symmetric solution

$$u_r \sim r^{\lambda_2+1} \cos \lambda_2 \theta \cos k\varphi, \quad (3.42)$$

is equal to  $\lambda_2 = 6$  which is in agreement with the prescribed inequality. This implies that the radial velocity has the same sign in the  $r, \theta$ -plane for a constant  $\varphi$ -value. We can conclude that in three dimensions, if the angle is smaller than the critical value, no eddies will occur near the rim. The fluid flow will be dominated by the flow in  $\varphi$ -direction. Note that this solution is not singular.

#### 4. CONCLUSIONS

In this paper, we have derived solutions for the fluid flow near corners and rims. For two- and three-dimensional geometries analytical descriptions of the velocity-components are constructed. For two- as well as three-dimensional geometries singular solutions can be found for angles  $2\gamma > \pi$ .



In two dimensions, an infinite sequence of eddies will occur in wedges with  $2\gamma < 2\gamma_e$ , which appears in the analytical formulation as complex eigenvalues.

For the three-dimensional solutions, Fig. 4 shows the real part of the smallest eigenvalues  $\lambda_2$  and  $\lambda_3$  plotted as a function of the angle  $2\gamma$ . The dash-dotted line indicates that the eigenvalues  $\lambda_3$  are complex. When a circular rim of an obstacle has an axisymmetric angle in the  $r, \theta$ -plane smaller than  $2\gamma_c$ , the fluid flow near the circular rim can be described by (3.41). We can conclude that eddy structures can only show up in geometries with  $2\gamma_c < 2\gamma < 2\gamma_e$ .

We illustrate the difference in particle tracks for some geometries with different corner angles  $2\gamma$ . An illustrative drawing of the particle track in laminar flow near a sharp rim is given by Fig. 5. In this figure,  $2\gamma = \pi/2$ . We can see that the particle swirls around the object. In Fig. 6 scaled particle tracks are computed with (3.13) for three corner angles. The tracks are computed with a four-stage explicit Runge-Kutta scheme. Fig. 6a shows the swirling for the corner angle  $2\gamma = \pi/2$ , which lies between  $2\gamma_c$  and  $2\gamma_e$ . It can be observed that the dominant behavior of the particle track is given by (3.33). Fig. 6b shows a particle track which goes through the same point (denoted with a P in the figures) for a corner angle  $2\gamma = \pi/4$ , which is just a little bit smaller than the critical angle  $2\gamma_c$ . The swirling behavior has disappeared, but there is still an influence noticeable of the swirling terms in (3.13). Fig. 6c shows the particle track for a corner angle  $2\gamma = \pi/8$ . In this case it is clear that the dominant behavior of the particle is given by (3.41). For the case of flow over a circular orifice of infinitesimal thickness, which corresponds to  $2\gamma = 2\pi$ , the analytical solutions have been computed in literature [3, 15]. The lowest order solutions for the velocity components we found vary as  $r^{1/2}$  which agree with [15].

## Acknowledgement

This work was supported by STW, the Netherlands Technology Foundation, under project TWI44.3286. The authors wish to thank Prof. P.J. Zandbergen and Dr. H.K. Kuiken for stimulating discussions and recommendations.

## REFERENCES

- [1] X. Bohou. Some problems in slow viscous flow. Technical report, The Danish Center for Applied Mathematics and Mechanics, 1985.
- [2] P. Burda. On the corner singularities of the Stokes flow in axisymmetric domains. *Z. angew. Math. Mech.*, 78:S319–S320, 1998.
- [3] A.M.J. Davis. Shear flow disturbance due to a hole in the plane. *Phys. Fluids A*, 3:478–480, 1991.
- [4] J.M. Dorrepaal, M.E. O’Neill, and K.B. Ranger. Axisymmetric Stokes flow past a spherical cap. *J. Fluid Mech.*, 75:273–286, 1976.
- [5] C.H. Driesen and J.G.M. Kuerten. An accurate boundary-element method for Stokes flow in partially covered cavities. To be published, also available as *Memorandum No. 1442*, University of Twente, The Netherlands, 1998.
- [6] C.H. Driesen, J.G.M. Kuerten, and M. Streng. Low-Reynolds-number flow over partially covered cavities. *J. Eng. Math.*, 34:5–20, 1998.
- [7] H. Hasimoto. Low Reynolds number shear flow along a circular hole. *J. Phys. Soc. Jpn.*, 50:3521–3524, 1981.
- [8] M.A. Kelmanson. Modified integral equation solution of viscous flows near sharp corners. *Computers & Fluids*, 11:307–324, 1983.
- [9] H.J. Lugt and E.W. Schwiderski. Flows around dihedral angles. *Proc. R. Soc. Lond. A*, 285:382–399, 1965.
- [10] D.H. Michael and M.E. O’Neill. The separation of Stokes flows. *J. Fluid Mech.*, 80:785–794, 1977.
- [11] H.K. Moffatt. Viscous and resistive eddies near a sharp corner. *J. Fluid. Mech.*, 18:1–18, 1964.
- [12] H.K. Moffatt and B.R. Duffy. Local similarity solutions and their limitations. *J. Fluid Mech.*, 96:299–313, 1980.
- [13] C. Pozrikidis. *Boundary Integral and Singularity Methods for Linearized Viscous Flow*. Cambridge University Press, New York, 1992.
- [14] C. Pozrikidis. Shear flow over a plane wall with an axisymmetric cavity or a circular orifice of finite thickness. *Phys. Fluids*, 6:68–79, 1994.
- [15] C. Pozrikidis. Shear flow over a protuberance on a plane wall. *J. Eng. Math.*, 31:29–42, 1997.

**Figure captions**

Figure 1: Definition of  $r$ ,  $\theta$  and  $\gamma$ .

Figure 2: The vorticity  $\frac{\partial v}{\partial x} - \frac{\partial u}{\partial y}$  plotted around a corner.

Figure 3: Definition of  $r$ ,  $\theta$ ,  $\varphi$  and  $a$ .

Figure 4: The real part of the smallest eigenvalues  $\lambda_2$  and  $\lambda_3$  as a function of the angle  $2\gamma$ . The dash-dotted line indicates that the eigenvalues are complex.

Figure 5: An illustration of a particle moving along a sharp rim.

Figure 6: Particle tracks for a particle moving along a sharp rim for  $2\gamma = \pi/2$  (**a**),  $2\gamma = \pi/4$  (**b**), and  $2\gamma = \pi/8$  (**c**). The particle tracks are scaled. The dash-dotted lines are the projections of the particle tracks on the surface  $x = -2$ . In every figure, the particle flows through the point P. Definition of  $r$ ,  $\theta$  and  $\gamma$ .

FIGURE 1

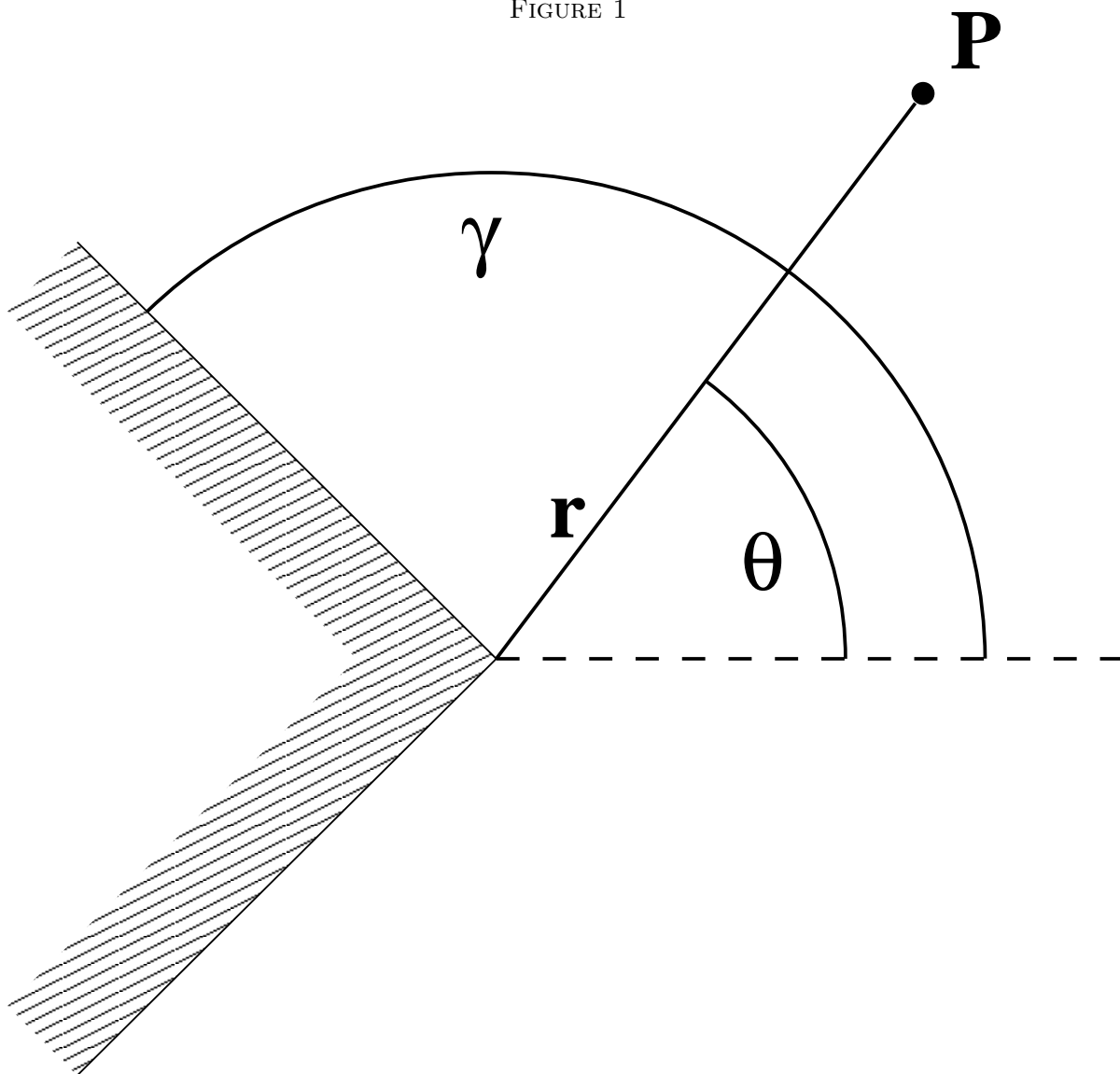


FIGURE 2

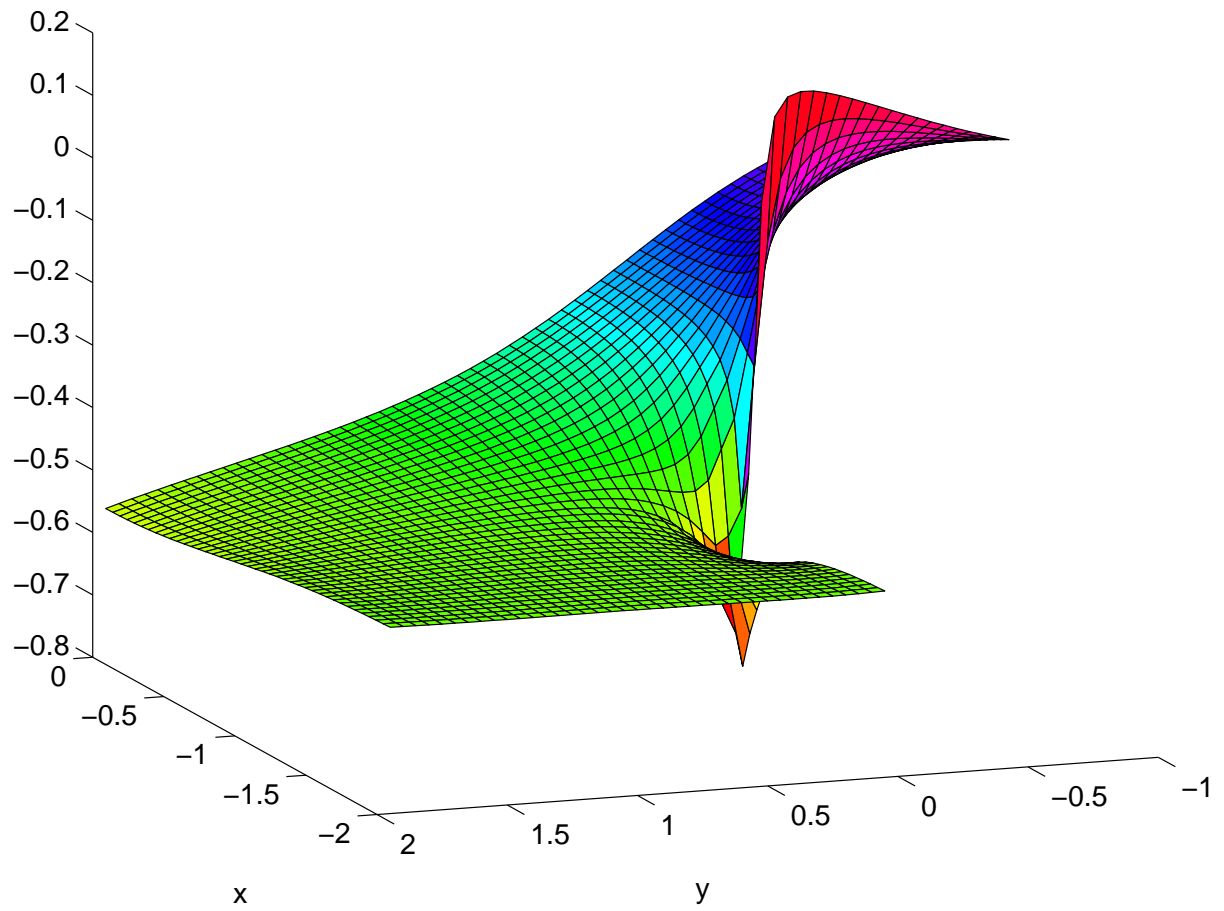


FIGURE 3

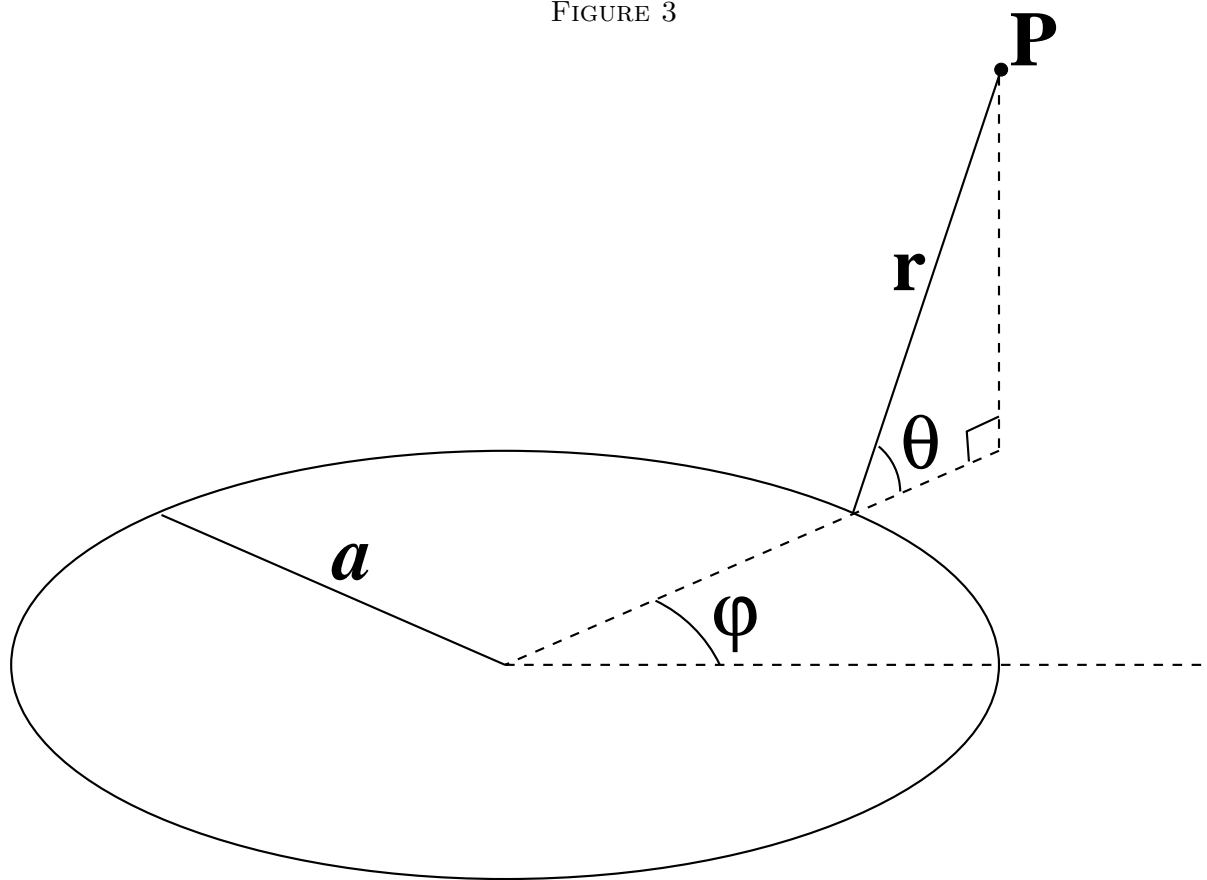


FIGURE 4

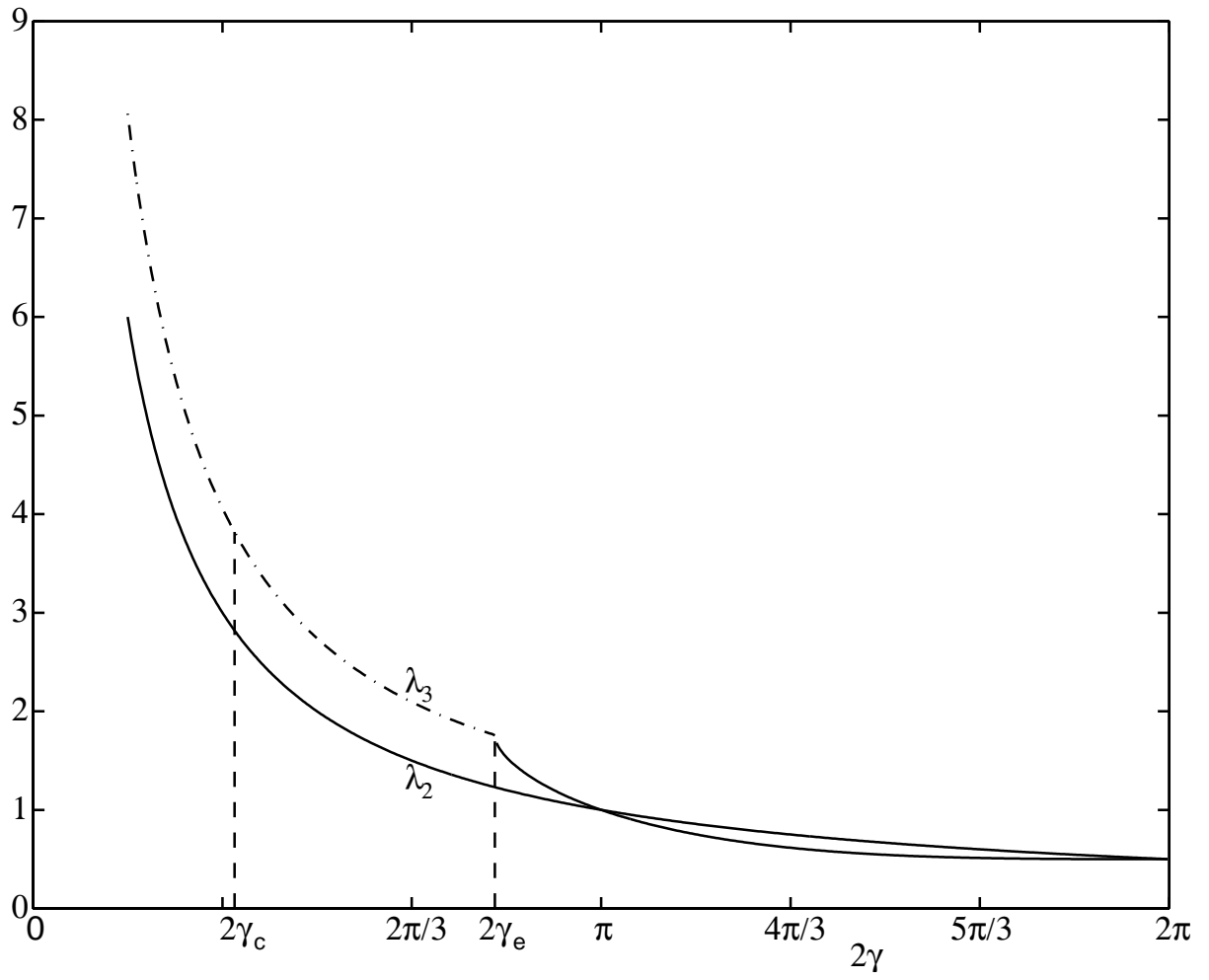




FIGURE 5

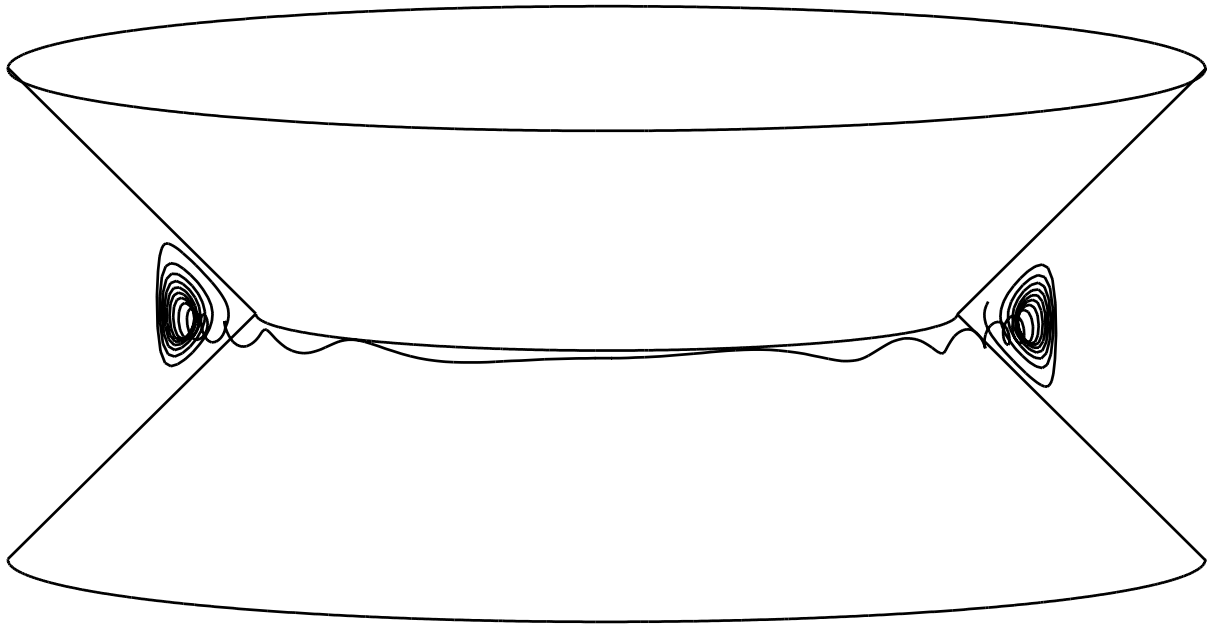


FIGURE 6

